ponents give temperatures of 2.6×10^4, 1.1×10^5, and 4.6×10^5 K. The total density for this distribution is $\sim 100\ cm^{-3}$. All the measurements in the dense plasma tail (1101:20 to 1103:20 U.T.) were made in the normal mode, with energies extending down to only 10 eV. Obtaining accurate Maxwellian fits to the part of the distribution with lowest energy becomes a problem at these low temperatures without data points extending to lower energy values. In particular, if the plasma tail electron temperatures should fall to even lower values than in the adjacent inner coma where our photoelectron mode spectra were obtained, the calculated densities will be too low and total integrated temperatures too high. The intermediate distribution, shown in Fig. 9, found in the comet's cold intermediate coma may represent the electrons in the 20- to 30-eV energy range that are produced by photoionization of cometary molecules (*16*).

The plasma tail region in the center of the intermediate coma was exceptionally well defined (Fig. 7). With a single encounter it is not possible, of course, to determine the exact configuration of the dense plasma region, but since a two-lobed magnetic tail with neutral sheet was observed at the comet (*7*), this enhanced plasma may be the plasma or current sheet required in such a field-reversing magnetic topology. It may have a flattened slab or sheet configuration separating the two lobes, similar to the current sheet at Venus and the plasma tail in Earth's magnetotail. In the center of the plasma tail at Giacobini-Zinner we would expect to find an embedded neutral sheet. The enhanced density in the developing plasma tail should lead to decreased magnetic field strength through the diamagnetic effect.

In summary, the ICE encounter with comet Giacobini-Zinner revealed a strong solar wind–cometary plasma interaction. Many of the regions of the cometary tail postulated by theory were detected, but no evidence of a small-scale standing bow shock was found at the encounter distance behind the nucleus. Future explorations would be required to determine if a shock exists, for example, closer to the subsolar point of this comet. A recent study suggests that a bow shock might be absent on the flanks of a comet (*17*). We see evidence in the plasma electron data for electromagnetic instabilities associated with cometary ion pickup, possible cometary ray or streamer structures, the comet's cold intermediate coma surrounded by a boundary layer, and a developing cold plasma tail that is thought to be required by the draping magnetic topology. Other features of the comet, such as the existence of a contact surface, may emerge from future analyses of combined plasma and field data. We would expect the contact surface to be associated with the region that we have called a boundary layer.

REFERENCES AND NOTES

1. S. J. Bame *et al., IEEE Trans. Geosci. Electron.* **GE-16**, 160 (1978).
2. M. D. Montgomery, J. R. Asbridge, S. J. Bame, *J. Geophys. Res.* **73**, 4999 (1968).
3. K. W. Ogilvie, J. D. Scudder, M. Sugiura, *ibid.* **76**, 8165 (1971); W. C. Feldman, J. R. Asbridge, S. J. Bame, M. D. Montgomery, *ibid.* **78**, 3697 (1973).
4. S. J. Bame *et al., ibid.* **85**, 2981 (1980).
5. M. K. Wallis, *Nature (London)* **233**, 23 (1971).
6. N. F. Ness and B. D. Donn, *Mem. Soc. R. Liege Vol. Hors Ser. 5* **12**, 141 (1965).
7. E. J. Smith *et al., Science* **232**, 382 (1986).
8. H. Alfvén, *Tellus* **9**, 92 (1957).
9. C. T. Russell, J. G. Luhmann, R. C. Elphic, F. L. Scarf, *Geophys. Res. Lett.* **8**, 843 (1981); C. T. Russell, J. G. Luhmann, R. C. Elphic, M. Neugebauer, in *Comets*, L. L. Wilkening, Ed. (Univ. of Arizona Press, Tucson, 1982), p. 561; D. J. McComas, H. E. Spence, C. T. Russell, M. A. Saunders, *J. Geophys. Res.*, in press; J. A. Slavin, D. S. Intriligator, E. J. Smith, unpublished manuscript.
10. S. J. Bame, J. R. Asbridge, H. E. Felthauser, R. A. Olson, I. B. Strong, *Phys. Rev. Lett.* **16**, 138 (1966); S. J. Bame, J. R. Asbridge, H. E. Felthauser, E. W. Hones, I. B. Strong, *J. Geophys. Res.* **72**, 113 (1967); N. F. Ness, *ibid.* **70**, 2989 (1965).
11. W. F. Huebner, P. T. Giguere, W. L. Slattery, in *Comets*, L. L. Wilkening, Ed. (Univ. of Arizona Press, Tucson, 1982), p. 496.
12. H. U. Schmidt and R. Wegmann, *ibid.*, p. 538.
13. K. Wurm, *Astron. J.* **66**, 362 (1963).
14. W.-H. Ip and W. I. Axford, in *Comets*, L. L. Wilkening, Ed. (Univ. of Arizona Press, Tucson, 1982), p. 588.
15. N. Meyer-Vernet *et al., Science* **232**, 370 (1986).
16. J. S. Lee, J. P. Doering, T. A. Potemra, L. H. Brace, *Planet. Space Sci.* **28**, 973 (1980).
17. M. K. Wallis and M. Dryer, *Nature (London)* **318**, 646 (1985).

18. We thank P. Corrigan and R. Wales and other members of the ICE project staff for pleasant and professional support during this remarkable third phase of the International Sun-Earth Explorer 3 mission. Without the ingenious and remarkable peregrinations of ICE devised by R. Farquhar, this mission would never have happened. The science planning, headed by project scientist T. von Rosenvinge, made our participation in the mission a pleasure. We also appreciate the support of our Los Alamos co-workers, particularly S. Kedge and J. Goetzinger.

20 November 1985; accepted 31 January 1986

Observations of Energetic Ions from Comet Giacobini-Zinner

R. J. Hynds, S. W. H. Cowley, T. R. Sanderson, K.-P. Wenzel, J. J. Van Rooijen

During the encounter with comet Giacobini-Zinner, the energetic particle anisotropy spectrometer on the International Cometary Explorer spacecraft observed large fluxes of energetic ions, believed to result principally from ionization of the cometary atmosphere followed by pickup and acceleration by the ambient flow of the solar wind. These heavy cometary ions were observed from approximately 1 day before closest approach to about 2½ days afterward. Three regimes of differing ion characteristics have been identified. An outer region with a scale of $\sim 10^6$ kilometers contains variable fluxes of antisolar-streaming pickup ions in the undisturbed solar wind. In the middle region, of $\sim 10^5$ kilometers, fluxes have less large-scale variability and broader angular and energy distributions. This region is separated from the outer zone by a sharp transition. The inner region has a scale of $\sim 10^4$ kilometers and is characterized by reduced fluxes and complex angular distributions.

More than 20 years have passed since it was predicted that the interaction between a cometary atmosphere and the solar wind would result in the production of large fluxes of energetic heavy ions in a large volume surrounding the nucleus of the comet (*1, 2*). Neutral atoms and molecules sublimating from the cometary nucleus expand outward, unrestrained by any significant gravitational attraction, at speeds of ~ 1 km sec^{-1}. They are then photoionized by solar ultraviolet radiation or by charge exchange with solar wind ions on characteristic time scales of $\sim 10^6$ seconds, creating an ion distribution extending $\sim 10^6$ km around the comet. On ionization, the newly created ions start cycloidal motion in the crossed electric and magnetic fields of the solar wind, thereby gaining energy proportional to their mass. For typical solar wind velocities the maximum energy gain is a few kiloelectron volts per atomic mass unit. Thus, for an ion in the "water group" (O^+, OH^+, and H_2O^+), expected to be the predominant ions, peak energies of some tens of kiloelectron volts are to be expected.

Acceleration of these heavy ions extracts energy from the solar wind plasma, so that,

R. J. Hynds and S. W. H. Cowley, Blackett Laboratory, Imperial College, London SW7 2BZ, United Kingdom.
T. R. Sanderson and K.-P. Wenzel, Space Science Department of European Space Agency, European Space Research and Technology Centre, Noordwijk, Netherlands.
J. J. Van Rooijen, Space Research Laboratory, Sterrekundig Institute, Utrecht, Netherlands.

when sufficiently close to the comet nucleus, where the mass density of these "pickup" ions approaches that of the ambient plasma, the solar wind flow becomes mass-loaded and its speed is significantly reduced. The distance at which this condition is reached defines the dimension of the large-scale interaction between the cometary atmosphere and the solar wind. However, clearly observable fluxes of heavy pickup ions should occur outside this region as well.

We present here an initial assessment of the observations of energetic heavy ions observed by the energetic particle anisotropy spectrometer (EPAS) on the International Cometary Explorer (ICE) spacecraft during its flyby of comet Giacobini-Zinner in the period 10 to 13 September 1985.

The EPAS measures ions in eight logarithmically spaced energy channels, data from the lowest five of which are reported here. For protons the ranges of these channels are 35 to 56.5, 56.5 to 91, 91 to 147, 147 to 238, and 238 to 384 keV (*3*), but due to pulse height defect effects in the semiconductor detectors these ranges depend on ion mass. For water group ions, believed to be the predominant species measured here, the results of Ipavich *et al.* (*4*) lead to the following provisional energy ranges: 65 to 95 (E1), 95 to 140 (E2), 140 to 205 (E3), 205 to 310 (E4), and 310 to 480 (E5) keV.

The system consists of three identical particle telescopes, inclined at independent angles (30°, 60°, and 135°) to the spacecraft spin axis, the latter pointing northward and maintained perpendicular to the ecliptic plane. As the spacecraft spins, the output from each telescope in each energy channel is binned into one of eight equiangular (45°) sectors, with sector 1 detecting particles from the solar direction and sector 3 detecting particles from east of the spacecraft-sun line. This combination of three telescopes, eight sectors, and eight energy channels enables EPAS to measure the three-dimensional ion distribution around the spacecraft. Each telescope accepts ions within a cone with a half-angle of 16° and has a geometrical factor of 0.05 $cm^2\ sr^{-1}$. Counts are accumulated over an integral number of spacecraft spin periods; during the cometary encounter the average temporal resolution was 32 seconds. The instrument is not able to resolve ion species.

Overview of the EPAS observations. Energetic ions produced by the interaction between comet Giacobini-Zinner and the solar wind were observed over an extended interval around the point of closest approach, initially approximately 1 day before encounter (at a distance of $\sim 1.8 \times 10^6$ km), and subsequently for about 2½ days afterward (at $\sim 4 \times 10^6$ km). This represents the first direct detection of cometary charged particles. The ions were observed to be streaming predominantly in the antisolar direction, such that peak fluxes were usually (although not invariably) recorded by telescope 2 in sector 1. Figure 1 shows 256-second averages of these fluxes for the lowest four energy channels during 10 to 13 September 1985. Large fluxes of energetic ions were observed that showed an overall peak near to closest approach at 1102 universal time (U.T.) on 11 September, although there was a marked dip in the region of the comet tail. The fluxes generally decreased on either side of the peak, though with a marked asymmetry between inbound and outbound passes (to the south and north of the comet, respectively).

At their peak, the counting rates were comparable to the largest rates previously observed by EPAS, either in the vicinity of interplanetary shocks or in the geomagnetic tail. Ions were also observed with energies exceeding 300 keV (assuming water group or heavier ions), although these were generally confined to the central part of the encounter, within 1.5 hours of closest approach.

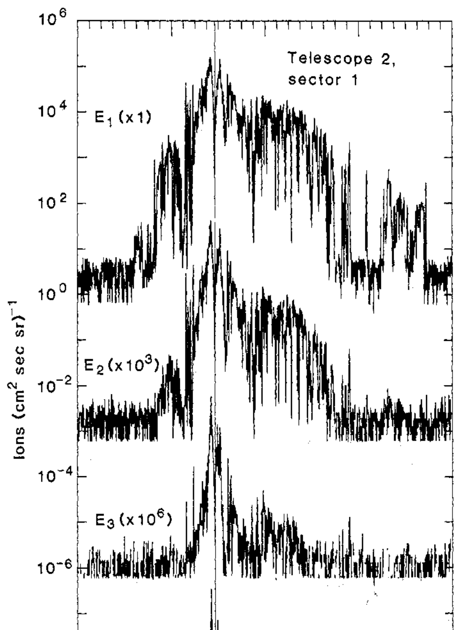

Fig. 1. Fluxes in the lowest four energy channels of telescope 2, sector 1, for 10 to 13 September 1985 (256-second averages). The flux scale on the left applies to energy channel 1, while the fluxes in the higher energy channels have been scaled to avoid overlap. Closest approach to the comet occurred on 11 September at 1102 U.T.

We now consider the nature and source of the measured ions, remembering that EPAS cannot directly resolve particle species. We believe that the energetic ions detected are heavy ions originating from ionization of the extended neutral comet atmosphere, followed by pickup and energization by the ambient solar wind flow. This is a simple and physically plausible way of producing antisolar-streaming ions in the 10- to 100-keV range, given initial neutral atoms or molecules of a few tens of atomic mass units, although additional processes (such as compression and diffusion) may be required to account for the ions of highest energy in the inner regions. Acceleration of solar wind protons to comparable intensities and energies by, for example, a cometary bow shock, raises serious difficulties, and it would also then be difficult to account for the predominant antisolar-streaming direction. Identification of the main heavy-ion species observed will require detailed comparisons between energetic ion and thermal plasma data. Ogilvie *et al.* (*5*) found that the predominant ions at somewhat lower energies in the vicinity of the comet do indeed belong to the water group. In addition, Ipavich *et al.* (*6*) were able to infer from their results the presence of water group ions that fall in the energy range of the EPAS instrument.

Examination of the ion data shows the existence of three distinct regimes. First, we have an outer region characterized by highly collimated antisolar-streaming ions with large, irregular variations in intensity. Then there is a middle region extending to 1.5 hours on either side of the closest approach where the ion distributions are much broader, both in energy and in angle, and where the overall intensity levels vary more smoothly, although with considerable point-to-point variability. Finally, there is a 20-minute-wide region occupying the central part of the encounter, characterized by reduced flux levels and complex, variable angular distributions. In general terms, we identify the outer region with the zone of $\sim 10^6$ km where observable energetic heavy ion production occurs in the undisturbed solar wind, while the middle region of $\sim 10^5$ km corresponds to the turbulent "mass-loading" regime where substantial slowing of the solar wind was observed (*5, 7*). The inner region then corresponds to the cold ion tail and induced magnetotail regions, having cross-tail dimensions of $\sim 10^4$ km (*7–9*).

The region of pickup ions in the solar wind. Pickup ions were observed in the solar wind for approximately 1 day before closest approach and for about 2½ days afterward (Fig. 1). The ions arrived from the solar direction and were observed predominantly in sector 1 of telescope 2 (inclined 30° to the ecliptic plane), although on occasion the peak fluxes did shift to an adjacent azimuthal sector of telescope 2, and sometimes the peak was observed by telescope 3.

The characteristic feature at distances remote from the comet was the appearance of bursts of particles, with the intensities increasing and then decreasing by one or more orders of magnitude on time scales of 10 to 20 minutes. More extended intervals of increased intensity did occur, and near the comet measurable fluxes existed between bursts. However, both peak and trough intensities generally declined with increasing distance from the comet (Fig. 1), so that eventually trough intensities dropped below the background level and ions were detected only in the peaks.

Several low-intensity bursts were observed in the early part of 10 September, the first between 1050 and 1054 U.T., but the first major increase occurred at 1934 to 1948 U.T. This activity continued as ICE approached the comet, culminating in four very intense peaks at 0342, 0415, 0451, and 0534 U.T. on 11 September. After this last burst, fluxes remained high and continued to increase as the comet approached.

A typical example of the ion behavior in the pickup region is given in Fig. 2, which shows the omnidirectional flux (spin- and telescope-averaged) at 32-second resolution, for energy level 1. The time interval shown is from 1200 to 1500 U.T. on 11 September 1985, when the spacecraft was outbound from the comet. We consider first the pickup region interval from 1300 to 1500 U.T. During this interval several variations of one order of magnitude occurred, variations that were seen predominantly by telescope 2 (nearest to the ecliptic). The azimuthal distributions observed by this telescope in energy channel 1 are indicated by the insets at the top of Fig. 2, taken at the times arrowed in the flux plot—one within a burst, the other immediately outside. These distributions are displayed such that the count rates for antisunward-moving particles are plotted upward and the count rates for westward-moving particles are plotted to the left. Fluxes are shown on a linear scale, with each plot normalized to the peak flux in that plot. So that intensities may be compared, the peak flux is labeled by the number of counts recorded in the sample (to convert to ions per square centimeter per steradian per second, multiply by 5). These angular distributions clearly show that, during this interval, the fluxes arrived predominantly from the solar direction, both inside and outside the burst.

It is difficult to understand the burst structure in terms of structure in the parent neutral distribution. Consideration of the pickup process in the solar wind, however, offers a simple and consistent hypothesis. The peak energy on the cycloidal orbits of pickup ions of mass A amu is given by

$$E_{max} = 4A \ \sin^2 \alpha \, E_{sw}$$

where E_{sw} is the energy of a proton traveling at the solar wind bulk speed and α is the cone angle between the solar wind velocity vector and the magnetic field direction. Thus the peak energy depends on the magnetic field direction as well as the solar wind velocity, while the direction of motion due to the $E \wedge B$ drift also depends on the direction of B. However, if efficient pitch angle scattering occurs in the flow rest frame, then the peak energy of the ions is $4AE_{sw}$ irrespective of field direction and the mean direction of motion depends only on the direction of the solar wind flow.

In the period represented in Fig. 2, preliminary data show that the solar wind velocity was relatively constant (*7*) but that there were fluctuations in the field direction (*8*). The sharp drop in flux at 1322 U.T. coincides with a field rotation from a northerly orientation to one that was almost radial (that is, α decreases). Other variations in flux level in Fig. 2 are also found to coincide with changes in the value of α. During an earlier period, 0830 to 0840 U.T. on 11

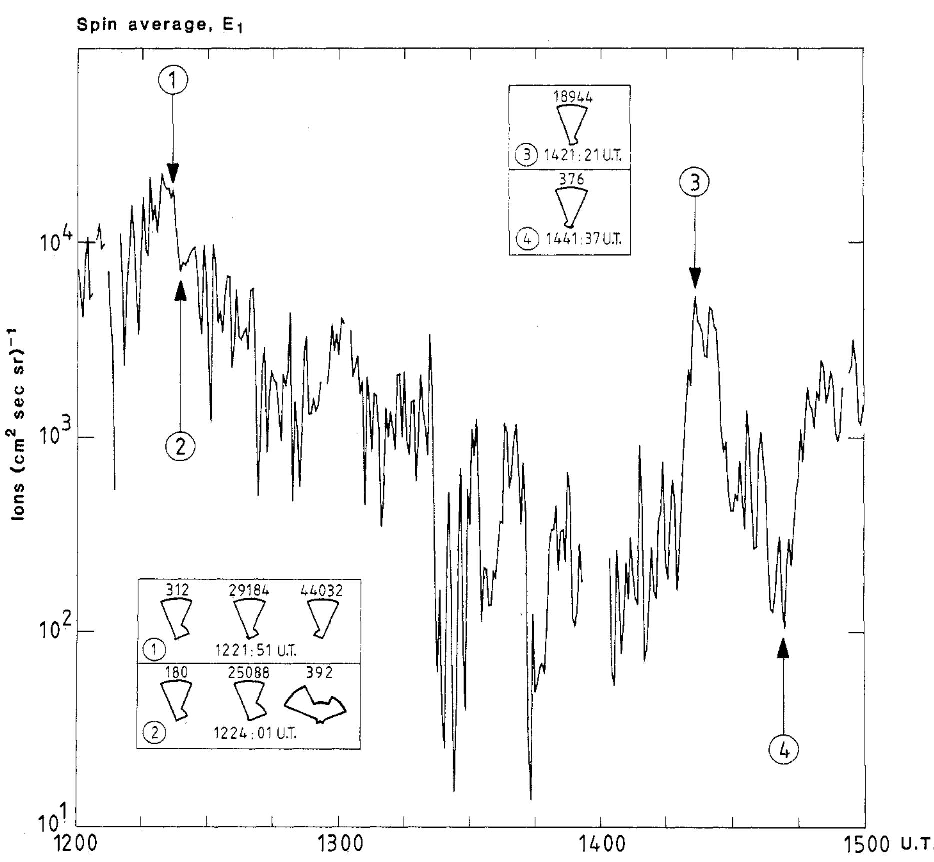

Fig. 2. Omnidirectional flux (spin- and telescope-averaged) for energy channel 1 during the interval 1200 to 1500 U.T. on 11 September 1985 (32-second data), showing the variability of the flux levels in the pickup region. Passage from the mass-loading to the pickup region occurred at 1223 U.T. The change in the angular distribution across this transition is indicated by sector plots (inset at lower left), measured in the 32-second intervals after the times indicated (see also arrows above). Azimuthal distributions are shown for telescopes 1 to 3 from left to right, and are plotted such that the count rates for antisunward-moving ions are plotted upward and the count rates for westward-moving ions to the left. Fluxes are plotted on a linear scale with each plot normalized to the peak sector in that plot. The number of counts in the peak sector is given to allow intercomparison of the fluxes observed by the three telescopes. The sector plots inset at the top show telescope 2 azimuthal distributions inside and outside an outer region burst, as indicated by the arrows beneath. The format is the same as before, except that telescope 1 and 3 fluxes are close to background at these times and are consequently not shown.

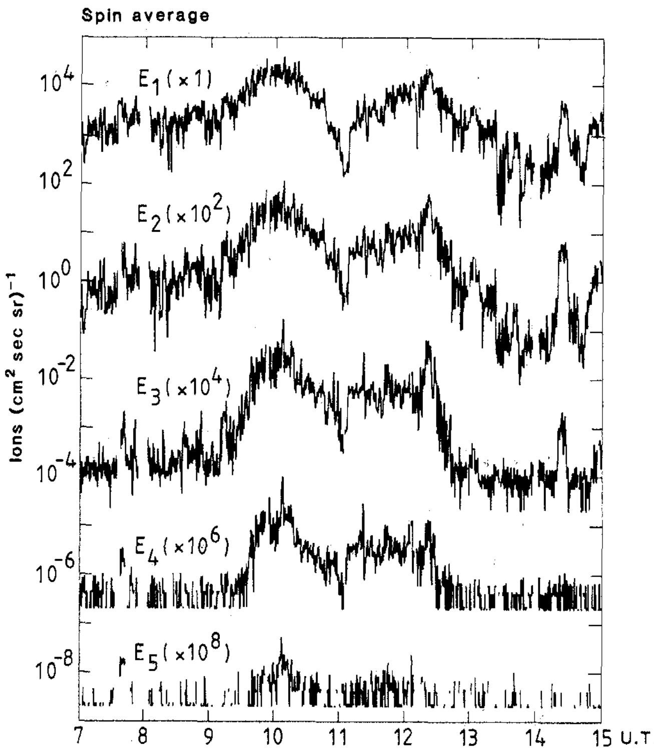

Fig. 3. Omnidirectional fluxes for the lowest five energy channels for the period 0700 to 1500 U.T. on 11 September 1985 (32-second intervals). Fluxes in the higher energy channels have been scaled in a manner similar to that in Fig. 1. The main inbound and outbound transitions between the pickup and mass loading regions occur at 0924 and 1223 U.T., respectively.

September, a strong southerly deflection of an "away"-pointing field occurred, which is expected to give rise to northward $E \wedge B$ drift. During this period, telescope 3 detected a large flux increase relative to telescope 2, which is completely consistent with the expected change in the direction of ion motion. Thus the variations in flux levels shown in Fig. 2 are consistent with changes associated with the magnetic field direction, although further analysis is required to confirm this. One implication of this hypothesis is that pitch angle scattering is not a dominant process in the pickup region, although some broadening of the ion distributions may occur.

Changes in ion flux levels associated with changes in solar wind flow speed also appear to be present. An increase in general flux level occurred across the large burst observed at 0534 U.T. on 11 September, and this coincides with an increase in solar wind speed from ~375 to 500 km sec^{-1} in the period 0520 to 0600 U.T. (*7*).

The overall changes in flux levels in the pickup region can be interpreted in gross terms as changes in ion source strength with distance from the cometary nucleus. More analysis is needed to determine whether the asymmetry between the flux levels observed during the inbound and outbound passages relative to the comet can be related to differences in solar wind flow and magnetic field characteristics, or whether an asymmetry in the cometary neutral cloud is also involved.

The mass-loading region. Figure 3 shows omnidirectional fluxes for the lowest five EPAS energy channels during the 8-hour period centered on closest approach to the comet (0700 to 1500 U.T., 11 September). This period encompasses the interval where the main thermal plasma and magnetic field effects were observed, involving slowing and heating of the flow and turbulence in, and draping of, the magnetic field (*7, 8*).

The gross changes in ion flux level during this period are the steady increase in flux in the lowest energy channel, which starts at 0920 U.T., peaks at 1010 U.T., and then declines as the comet is approached. After the point of closest approach, the flux level increases again relatively steadily until 1220 U.T., when the level drops sharply to values similar to those observed before 0920 U.T. At higher energies similar variations were observed, but with a much more pronounced initial increase and final decrease occurring near 0920 U.T. and 1220 U.T., respectively.

An important feature of the ion data in this region is that, overall, the fluxes observed by the three telescopes vary in magnitude rather slowly, and do not appear to be influenced by the magnetic field direction in the manner observed in the outer region. This suggests that the ions have become isotropized in the plasma rest frame and so respond primarily to changes in flow rather than to changes in magnetic field direction. It should be noted that it is within the mass-loading region that large fluctuations in plasma and field properties were also observed (*7, 8*), consistent with this suggestion. Indeed, despite the smooth overall behavior of the ion fluxes noted above, it is also clear from Fig. 3 that considerable point-to-point variations in flux level were also present in this region. Even at their peak, fluxes typically varied by factors of 2 to 5 over a few measurements (say, 2 to 3 minutes).

The transition from the pickup to the mass-loading region is relatively sharp in the ion data for both the inward and outward passages of the spacecraft. The largest effects were observed during the outbound transition, which occurred during the interval 1222:26 to 1223:30 U.T., as shown in the left-hand part of Fig. 2. Before the transition, large fluxes were observed in telescopes 2 and 3, with relatively little in telescope 1, indicating plasma flow to the north, while after the transition fluxes in telescope 3 were much reduced, to levels comparable with those in telescope 1. These changes are illustrated in the lower inset in Fig. 2, where azimuthal distributions for all three telescopes are plotted (energy channel 1) for two 32-second intervals, one just before the transition and one just after. In general, inside the transition the ion distributions are broader in angle (and energy) than in the pickup region.

A similar, but less marked transition also occurred on the inbound pass between 0924:23 and 0924:55 U.T. when there was an increase in flux of one order of magnitude in telescope 1, while fluxes in telescopes 2 and 3 remained relatively unchanged. Farther inbound from the transition, fluxes in telescope 1 continued to grow such that in the region of peak fluxes at 1000 U.T. the flux in telescope 1 considerably exceeded that in telescope 3, although it remained generally less than that in telescope 2. These distributions indicate a plasma flow deflected to the south.

The implication is that inside the transitions the flow is deflected away from the comet—inbound to the south and outbound to the north (ICE passes the comet in a south to north direction). The sharpness of the transitions suggests the presence of a shock, and we note that close to the outbound interval we have identified from the ion data, the plasma wave data (*10*) when analyzed show the characteristics of a shock. If shocks did occur, however, they must have been relatively weak in view of the small changes in plasma speed observed across them (*7*). The magnetometer did not observe a single sharp change in the field, but showed the appearance of large-amplitude field variations just inside the flow deflections (*8*).

The remaining part of the mass-loading region that needs to be considered is the decline in intensity about the point of closest approach, corresponding to an interval of about 90 minutes in Fig. 3. The origins of this decrease are not clear. One possibility is that energetic ions are removed by charge exchange with the dense inner neutral atmosphere of the comet, which would also cool the plasma flow. Within this inner part of the mass-loading region, examination of the ion angular distributions indicates that telescope 1 sees an increasing proportion of the flux on either side of the cold ion tail, with a bias toward a flow from the west in azimuth. This may be an anisotropy effect associated with the ion density gradient combined with draped magnetic field lines surrounding the comet tail.

The region of the cold ion tail. During the 20 minutes centered on 1102 U.T., the ICE spacecraft passed through the cold ion tail of the comet (*7, 9*), including the interior bipolar magnetic tail and embedded neutral sheet (*8*). Ion fluxes were much reduced in this region but still sufficiently high to provide satisfactory angular distributions. These distributions were much more complex than those obtained in the pickup and mass-loading regions, and probably reflect ion motion due to finite Larmor radius penetration from the high ion flux regions outside the cold ion tail.

Figure 4 shows the omnidirectional flux for the lowest energy channel during the interval 1030 to 1130 U.T., approximately centered on the closest approach to the comet at 1102 U.T. The approximate boundaries of the cold ion tail, the magnetic tail lobes, and the neutral sheet are shown at the bottom of Fig. 4 (*7–9*). The central "slot" of reduced flux corresponds closely to the location of the bipolar magnetic tail, and no increase of spin-averaged flux was observed in the neutral sheet.

The angular distributions in this central region show considerable variations in both zenith and azimuthal angles. The increasing proportion of the flux appearing in telescope 1 in the inner part of the interaction region culminates in a region in the outer part of the cold ion tail on either side where peak fluxes in telescope 1 exceed peak fluxes in telescope 2. In the central part of the bipolar magnetic tail and neutral sheet the situation reverts to the usual one in which telescope 2 observes the largest peak flux. Fluxes in telescope 3 remained lower than those in telescopes 1 and 2 throughout the tail region. Azimuthal distributions show more complex behavior. The distributions appearing in the inbound cold ion tail negative B_x lobe, neutral sheet, and initial high field strength positive B_x lobe are typified by the distribution at 1101:25 U.T. observed in the inner part of the negative B_x lobe (Fig. 4). Fluxes peaked in sector 2 in telescopes 1 and 2 (flow from the sun and from the east), while remaining peaked as before in sector 1 in telescope 3. The first distribution measured in the moderate field strength region of the positive B_x lobe showed different behavior, as also shown in Fig. 4 (1104:04 U.T. distribution). The angular distributions observed by telescopes 1 and 3 remained roughly the same as previously, while telescope 2 observed peak fluxes in sector 4 (flow sunward and from the east). Similar distributions were observed until 1109:56 U.T., when antisunward-directed fluxes reappeared in telescope 2, and later in telescope 1, although telescope 3 then began to observe peak fluxes directed toward the sun. Later, from 1112:36 to 1114:44 U.T., all three telescopes observed the peak intensity flowing toward the east. After this the distribution reverted to becoming dominated by flow directed from the sun, and remained so thereafter.

Summary. During the encounter of the ICE spacecraft with Giacobini-Zinner, the EPAS instrument measured large fluxes of energetic ions that we believe to be heavy ions of cometary origin, created in situ in the surrounding solar wind plasma and consequently accelerated by the solar wind flow. These ions were observed for approximately 1 day before the encounter and for about 2½ days afterward (corresponding to distances of $\sim 1.8 \times 10^6$ and $\sim 4 \times 10^6$ km).

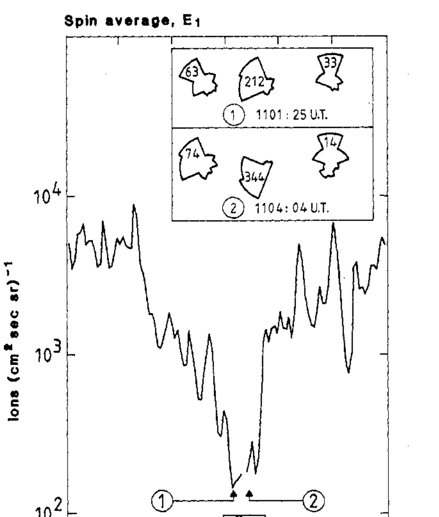

Fig. 4. Omnidirectional fluxes for energy channel 1 for the interval 1030 to 1130 U.T. on 11 September 1985 encompassing the ICE passage through the comet's cold ion tail and induced magnetotail, approximate locations of which are indicated at the bottom. The sector plots (inset) show two representative angular distributions measured in the 32-second intervals following the times indicated, in the format of Fig. 2 (see also the arrows in the flux plot).

The properties of the observed ions identify three distinct regions corresponding to the pickup region in the undisturbed solar wind (scale size, $\sim 10^6$ km), the mass-loading interaction region ($\sim 10^5$ km), and the cold ion and magnetic tail (cross-tail scale size, $\sim 10^4$ km). In the solar wind the ion fluxes occur in bursts that appear to be controlled by the direction of the magnetic field, the solar wind flow speed, and the distance from the comet. These characteristics change across a sharp transition, indicative of a shock, located $\sim 10^5$ km from the comet, within which the flows appear to be deflected away from the comet. Inside this region the overall variation of the ion flux shows smoother behavior and does not respond strongly to changes in magnetic field orientation, as happens in the undisturbed region of solar wind. At the same time, considerable point-to-point changes are observed on time scales of a few minutes. From peak values at and inside the transition, omnidirectional fluxes then fall as the comet is approached, reaching minimum (but still observable) values within the high-field-strength bipolar tail lobes and embedded neutral sheet. Complex ion angular distribution changes were observed in this and in the surrounding cold-ion tail region.

REFERENCES AND NOTES

1. M. Harwit and F. Hoyle, *Astrophys. J.* **135**, 875 (1962).
2. L. Biermann, B. Brosowski, H. V. Schmidt, *Solar Phys.* **1**, 254 (1967).
3. A. Balogh *et al.*, *IEEE Trans. Geosci. Electron.* **GE-16**, 176 (1978).
4. F. M. Ipavich, A. Lundgren, B. A. Lambird, G. Gloeckler, *Nucl. Instrum. Methods* **154**, 291 (1978).
5. K. W. Ogilvie *et al.*, *Science* **232**, 374 (1986).
6. F. M. Ipavich *et al.*, *ibid.*, p. 366.
7. S. J. Bame *et al.*, *ibid.*, p. 356.
8. E. J. Smith *et al.*, *ibid.*, p. 382.
9. N. Meyer-Vernet *et al.*, *ibid.*, p. 370.
10. F. L. Scarf *et al.*, *ibid.*, p. 377.
11. The EPAS instrument was jointly produced by the Blackett Laboratory of Imperial College, the Space Research Laboratory, Utrecht, and the Space Science Department of the European Space Agency. We thank S. T. Ho and M. Szumlas for their assistance with data handling and the European Space Operations Centre staff for their support in transferring data from the Goddard Space Flight Center (GSFC) to the European Space Research and Technology Centre via the Space Physics Analysis Network. We also thank the ICE project team and the project scientist T. von Rosenvinge for their support before and during the comet encounter; W. Mish and his colleagues for enabling us to process our data at GSFC during the encounter period; and J. L. Green, J. H. King, and the staff in the National Space Science Data Center, GSFC, for assistance during the encounter.

20 November 1985; accepted 21 February 1986